Advances in Materials
2018; 7(4): 89-104
http://www.sciencepublishinggroup.com/j/am
doi: 10.11648/j.am.20180704.11
ISSN: 2327-2503 (Print); ISSN: 2327-252X (Online)

The X-Ray Diffraction Method for Study of Growth Defects in CVD Diamond Single Crystals

Andrzej Badzian

Materials Research Institute, Pennsylvania State University, University Park, U.S.A

Email address:
abadzian@psu.edu

To cite this article:
Andrzej Badzian. The X-Ray Diffraction Method for Study of Growth Defects in CVD Diamond Single Crystals. *Advances in Materials.* Vol. 7, No. 4, 2018, pp. 89-104. doi: 10.11648/j.am.20180704.11

Received: July 28, 2018; **Accepted**: October 11, 2018; **Published**: November 6, 2018

Abstract: X-ray diffraction from Chemical Vapor Deposition (CVD) gem-quality colorless diamond single crystals, grown with nitrogen addition in methane –hydrogen plasma mixture, was studied by imaging plate area detector (IPD) giving pixel pattern. Growth defects are responsible for rising x-ray diffuse scattering beyond reciprocal lattice points (rlp), described in the framework of kinematical theory of X-ray diffraction. In the particular case of CVD diamond crystals grown epitaxially on (001) substrate, the additional scattering in the close vicinity of rpl's was registered. This observation was possible because of the improved angular resolution of x-ray intensity measurements using imaging plate detector (IPD). The pronounced differences in scattering around 111 rlp's for natural and CVD <001> growth sector were demonstrated. Oscillation and stationary crystal methods allowed registration of diffraction spots that are different from natural diamond crystals. The diffraction patterns include features of short- and long-range atomic order. There are satellite reflections at the positions corresponding to the interatomic distances at 1.51 Å and 1.57 Å in the vicinity of 111 Bragg reflections, which are characteristic to 1.54 Å of cubic diamond. The displacement disorder of atoms, understood as disturbance of lattice periodicity can be explained by hypothesis about linear defects running in <110> and <-110> directions. Along <110> twin line tetrahedra share edges. Hydrogen atoms are presumably incorporated along this linear twin to protect chemical bonding stability. Bragg reflections exhibit anisotropy and considerable broadening compared to the diffraction standards. The ratio of peak intensity of forbidden by the diamond space group symmetry 222 reflection to 111 reflection is larger than for natural crystal. Raman spectra from (001) CVD crystals fit well to the spectrum from nearly perfect natural diamond crystal. The X-ray scattering around Bragg reflection is characteristic for a given crystal and can be applied as a gem quality criterion for distinguishing among crystals of different origin, or different growth sectors or grown by different methods. The scattering around 111 CVD diamond reflection is the strongest among the rlp's.

Keywords: Single Crystal Diamond, Microwave Plasma CVD, Defect Characterization, X-Ray Diffraction, Raman Spectroscopy, Scanning Tunneling Microscopy

1. Introduction

The X-ray diffraction patterns from CVD single crystals differ from those of natural diamond single crystals recognized as nearly perfect crystals. The growth defects disturb periodicity of CVD diamond crystal lattice.

None of growth processes (including the natural ones) allow growing ideal, flawless, single crystals. It is the consequence of the chaotic nature of growth processes. Non–equilibrium thermodynamics considers fluctuations as a source of growth defects.

Growth defects are responsible for rising x-ray diffuse scattering beyond reciprocal lattice points (rlp). [1] In the particular case of CVD diamond crystals grown epitaxially on (001) substrate additional scattering was registered in the close vicinity of rpl's. This observation was possible because of the improved angular resolution of x-ray intensity measurements using imaging plate detector (IPD). For example, the pronounced differences in scattering around 111 rlp's for natural and CVD <001> growth sector were demonstrated.

The present paper continues the recent study on IPD applications for CVD diamond materials [1]. Such study was focused on the comparison of natural diamond crystal with

CVD. The goal of present report is the description of IPD images from CVD diamond single crystals grown homoepitaxially on (001) substrates with nitrogen addition to CH_4/H_2 mixture in a microwave plasma. This x-ray diffraction approach can be extended for different CVD diamond crystals as a tool for characterization of single crystals.

There were many motivations for introduction of nitrogen gas during CVD diamond growth. It is a well-known finding that the presence of N_2 increases the rate of crystal growth and modifies their morphology in diamond and other materials. For example, Mierzejewska and Niemyski studied the influence of nitrogen and argon gases on boron deposition [2]. The addition of nitrogen increased the growth rate of boron ten times; however addition of argon did not affect the growth rate.

In diamond research, the early study of B-N-C system illustrates the difficulty to interpret the growth processes during CVD synthesis. [3, 4] The issue of C- N binary phases, popular in the 1800's, was revived in 1984 when Chin-Min-Sung of Norton-Christiansen, Salt Lake City, Utah, proposed synthesis of crystallographic analogue to $\beta - Si_3N_4$, as a material harder than diamond. This crystal chemistry concept ignited the whole new area of theoretical and experimental research, including CVD process explored by [5]. A mixture of CH_4 and N_2 gases was introduced to a silica tubular reactor. Microwave plasma was ignited in this reactor over graphite substrate. The process yielded disordered diamond nanocrystals. The growth rate was around 1 μm/ hour. Auger electron spectroscopy did not detect any nitrogen in this material due to detection limit. Raman spectrum was composed of two very broad maxima: one at cubic diamond position and the second one at 1500 cm^{-1}. Similar spectrum was described for highly oriented diamond (HOD) film on (001) Si [1]. This spectrum is a manifestation of a distinct phase with tetrahedral configuration confirmed by x-ray diffraction. X-ray diffraction powder pattern contained lines corresponding to cubic diamond, However, they were broad as a result of small crystal size and cubic lattice distortions [5]. At a different experimental setting, of methane/nitrogen mixture, a graphite-type binary C-N phase was formed. [6]. Also, N_2 addition during the growth of carbon nanotubes resulted in perpendicular stacking of graphitic planes within nanotubes. [7]

The influence of nitrogen gas concentration in methane and hydrogen mixture on the diamond growth has been studied in the range of 1- 1000 ppm. The enhancement of (001) type morphology and the increase of growth rate was observed at a few ppm of N [8]. These new growth phenomena led up to the development of a new single-crystal growth process. The increase of power of microwave generator was the critical step in this development, as well as finding proper location of the substrate under the luminous plasma ball [9]. There is an extensive literature on the development of single crystal growth on (001) diamond. These issues are not reported here.

The CVD diamond single crystals are available on the market as a result of decades of efforts undertaken by the enthusiasts of laboratory synthesis. According to the estimate made by Kitko Commentary in 2013 [10], the production of CVD gem quality diamonds was at a level of less than million carats. This corresponded to 2% of supply of gem quality crystals at this time, and it was predicted that "most likely (single crystals) will have a greater impact on technology than jewelry" [10]. This is an unbelievable success of the perseverance of generations of diamond researches. Many approaches have been proposed to grow diamonds, but we still don't know how natural diamonds were grown under the surface of the Earth and whether it is a hydrothermal process. [11] Microwave plasma process showed considerable advantages. First, gem quality CVD single crystal on (110) diamond substrate was assessed by The Gemological Institute of America in 1992 as 0.17 ct stone [12]. The crystal was shown in Life Magazine, March 1992.

Emerging applications of CVD diamond single crystals require proper characterization techniques. X-ray diffraction is a main characterization tool in this case. The easy penetration of X-rays throughout diamond crystal, high resolution and sensitivity of IPD are the critical advantages of this method. The other techniques like x-ray topography and double crystal diffractometry are also suitable in this case. This paper highlights the non-cubic features in x-ray diffraction patterns of diamond single crystals grown in the presence of N_2 and suggests a hypothesis about linear growth defects in <110> and <-110> directions as the explanation of these features.

2. Materials and Methods

Diamond single crystals, grown by microwave plasma CVD in the presence of N_2, and provided by Oriental Expression Jewelry Company, were studied by x-ray diffraction and Raman spectroscopy. Two groups of CVD samples were analyzed. One group had typical gem cutting, they were shipped from a jewelry store. The gems were colorless; some were water-clear, 2 mm of height, 0.2 carat of weight. The other group of CVD single crystals was 4x4 mm square plates (001), 2 mm thick. The square edges were along <110> and <-110> directions. These samples were cut off from the substrate of natural diamond (001) plates. Some crystals were light brown, some got polycrystalline inclusions on the top surface, and two crystals were extraordinary. The crystals have been provided by Dr. Bhandari. The extraordinary crystals had a brownish cross with arms oriented in the <110> and <-110> directions. The arms of the cross looked like bunches of thin numerous rods (threads). The diameter of these bunches was about 1 mm. We think that extraordinary process conditions allowed growing such crystals. The cross was located just under the surface, easy to observe with a naked eye. One single crystal plate was broken along (110) plane to get Raman spectra on it. The fractured surface showed lines of striation similar to

the observed ones for homoepitaxial CVD diamond films [12]. Three CVD crystals were studied using x-ray diffraction: 2 gem cut and one square plate. The gem samples were called "A" and "standard".

The x-ray diffraction (XRD) experiments followed oscillation and stationary crystal method and were conducted using RIGAKU D/MAX Rapid II x-ray diffractometer described in [1]. Raman spectra have been taken using Confocal Raman Microscope WITec alpha 300R.

Prompt-gamma activation analysis (PGAA) was applied to check the presence of nitrogen. Nitrogen was not detected by this method. The analysis was conducted by Dr. Lei (Raymond) Cao at the Center for Neutron Research, National Institute of Standards and Technology (NIST), Gaithersburg MD. The 10 crystals of CVD diamonds of total weight of 1.32g have been analyzed. The detector used at NIST facility detects 166 micrograms of N. So for analyzed sample the detection limit for N is 125ppm. No N signal from diamond crystals means that N level is below 125 ppm by weight.

3. Results and Discussion

3.1. Description of Scattering Around Rlp's

111 Rlp (8 Planes)

Oscillating crystal diffraction patterns were taken for rotation axis parallel to <110> direction of diamond crystal. Oscillation ranges Δω were chosen to detect the required reflections, when rlp passes across Ewald sphere. There are 8 reflections connected to {111} set of planes. These planes are equivalent, so reflections should have the same shape for single crystal of cubic structure. However, the registered CVD reflections are differed in shape and the extension of scattering around 111 rlps. The reported 111 reflections are arbitrarily chosen from {111} set. We recognized the differences as anisotropy of Bragg scattering in the reciprocal space.

The possible contributions to the scattering in the vicinity of rlp's were discussed in [1]. Now we consider the differences in scattering between CVD and natural single crystals. A natural crystal exhibited a single diffraction spot, which reflects rounded primary beam, while multiple spots appeared in CVD crystals.

The CVD reflections are broad with the extension larger then these for natural diamond. The {111} reflections are not identical. All oscillation reflections have maximum at cubic diamond 111 position as for Bragg reflection of natural crystal. There are two classes of CVD oscillation reflections. The first one is broad with one maximum at 111 of cubic diamond, and the second class has multiple maxima.

One broad CVD 111 reflection has width 1.75°2θ for crystal A and the other 111 for "standard crystal" has the width of 2.17°2θ at the base. We describe the broadening of the spots on horizontal level by the values of full width of intensity profile at 3 levels: at the half height of the intensity maximum (FW 0.5M), at 1% of maximum (FW 001M) and at 0.1% of maximum (FW 0.001M) to show the extension at the base of reflections. The borders of diffraction spot at horizontal line were measured in 2θ, and d_{111} values were calculated for such points. The spots for CVD crystals extend between d_{111} equal to 2.01Å and 2.10Å. We can assign these values to interatomic distances in tetrahedron in diamond unit cell. They are in the range between 1.51Å and 1.57Å, which corresponds to inter-atomic distances in equation (3) in [1].

In comparison, natural diamond spot extends between 44.557º and 43.363º 2θ, i.e. between d_{111} = 2.032Å and 2.085Å, or between 1.52Å and 1.56Å for interatomic distances. The width at 0.001M is 1.1°2θ, it means the 111 reflections are narrower. The calculated (111) maximum is assigned to d_{111}= 2.056Å, and corresponds to 1.544Å of inter-atomic distance in a regular tetrahedron in the diamond unit cell. The interatomic distances outside these values (152 Å and 156 Å) represent the displacement disorder of atoms, and are contained in the measured ranges of 2θ outside of natural diamond scattering. The broadening of reflections is a sign of deformation of tetrahedra.

The second group of reflections contains doublets and triplets. The structural doublets indicate the displacement of atoms at the specific inter-atomic distance, and have no relation to spectral doublets of CuK α1/α2. Structural doublets has, for example, 17 pixels resolution, whereas the spectral doublet has resolution of 2.5 pixel. The spectral doublet is not resolved in 111 spot. The other 111 reflections show clearly satellites located close to cubic diamond maximum. It is shown in Figure 1 and Figure 2. Instead of one maximum like in natural diamond, shown in [1], Figure 1, the oscillation pattern shows a satellite in the distance of 17 pixels from cubic diamond 111 Bragg maximum corresponding to the location of 111 rlp on the Ewald sphere. The image in Figure 1 has maximum at 44.138°2θ which corresponds to d_{111} = 2.049Å and to interatomic distance of 1.54Å. The profile of main maximum is shown below the spot image in Figure 1. The steps correspond to pixels, where 1 pixel has width of 0.045°2θ. We can calculate position of chosen pixel using 2θ positon of the main maximum and the number of pixels from the maximum. The position of satellite is 43.39°2θ. This position corresponds to d = 2.11Å. We can calculate position of chosen pixel using 2θ position of a main maximum and the pixel width. Rigaku software does not allow getting profile along the slant lines, only along the sides of pixel square. Determination of the second maximum requires separate verification of pixels. The satellite is at 43.39º (2.081Å) and its peak intensity is 17% of the main maximum height. This is a remarkable disturbance for cubic diamond diffraction pattern.

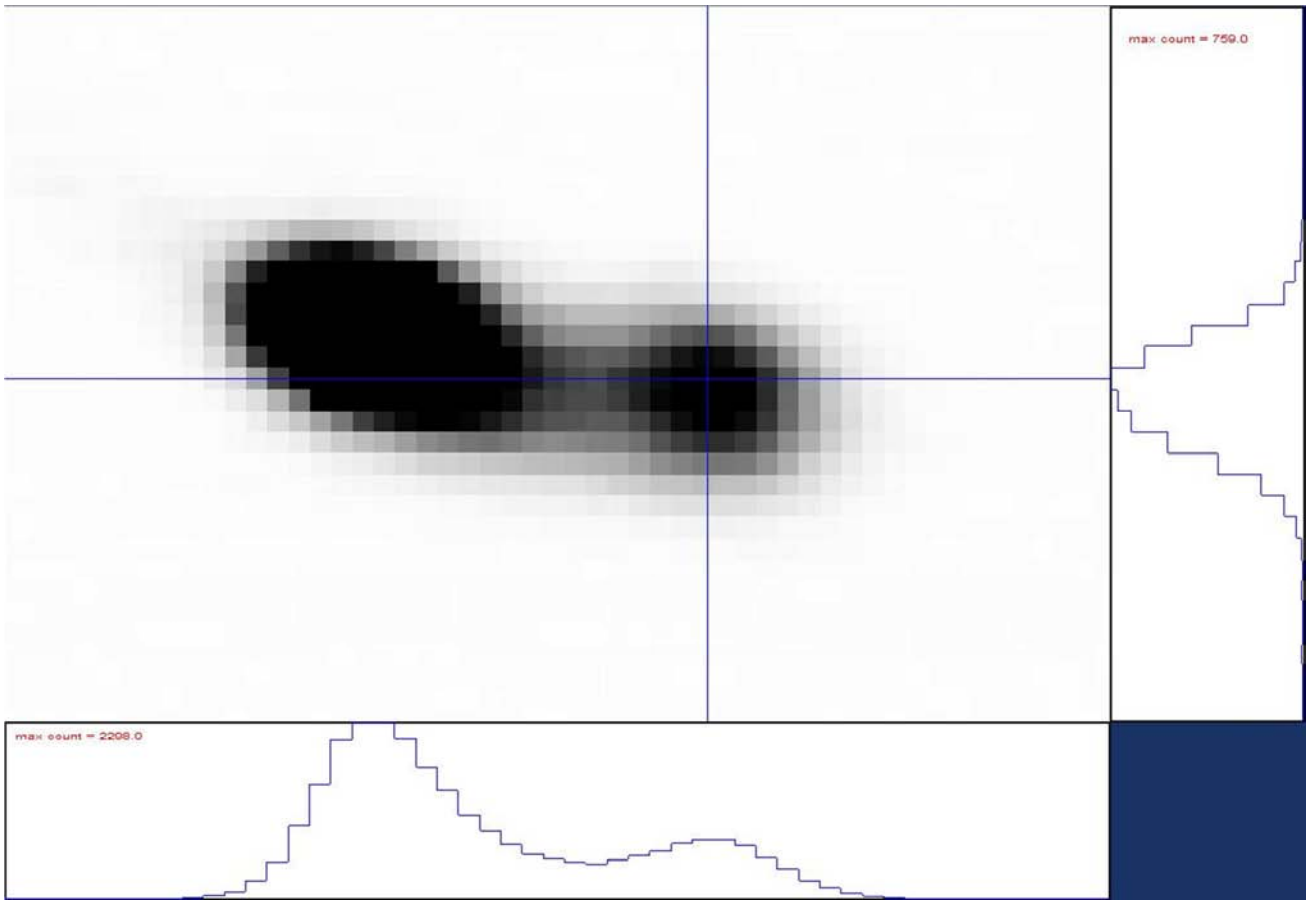

Figure 1. *Diffraction spot as structural doublet from "standard" CVD crystal, in the vicinity of 111 reciprocal lattice point. The crystal oscillation was within 10°ω. The stronger maximum is close to 111 Bragg reflection of cubic diamond at 44.12° 2θ. The satellite maximum is at 43.94° 2θ in the distance of 17 pixels on smaller θ angles. The intensity ratio of satellite to Bragg reflection maxima is 0.17.*

1.0°ω oscillation spot from crystal A with the 16 pixels resolution between main maximum and satellite is shown in Figure 2. The satellite shown in the center of the image has maximum at 43.25° 2θ (2.09Å) and shoulder towards smaller 2θ. The d_{111} extends to 2.10Å and further.

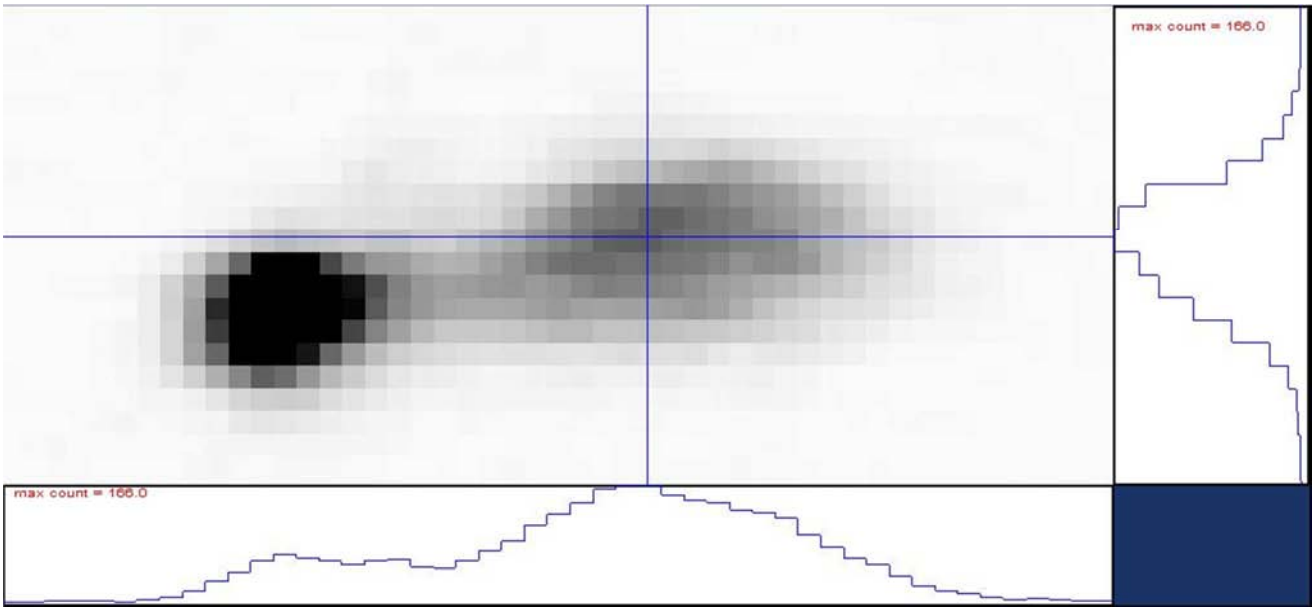

Figure 2. *Diffraction spots as doublet from crystal "A". The oscillation was within 1°ω. The stronger maximum at 43.95°2θ / 2.057Å corresponds to 111 Bragg reflection of diamond. The satellite maximum at 43.25° 2θ / 2.089 Å is in the distance of 16 pixels. The peak intensity ratio of satellite to Bragg 111 reflection is 0.2.*

The meaning of the satellite maxima relates to specific interatomic distances between the pairs of carbon atoms, which are preferred within the ensemble of atoms disturbed by disorder. The borders of diffraction spots with multiple maxima are similarly located like for the broad spot with one maximum. The difference between a broad spot and the spots with multiple maxima is in preference of specific inter-atomic distances within the range of displacement disorder. The most pronounced satellites are located around 2.08Å or 2.10Å (Figure 1 and 2), where natural diamond spot ends at 2.08Å, the CVD crystal has maximum of the satellite.

Stationary images bring additional information. Each stationary image obtained at a fixed ω angle constitutes a component of the oscillation profile, which integrates the scattered intensity within a chosen oscillation Δω range. Such component allows identification of non-cubic spots. However, no non-cubic spots for Si and natural diamond were found except at 311 rlp of natural diamond. This spot can have the origin similar to 222 forbidden reflection. The stationary images of scattering from CVD crystals in the vicinity of 111 rlp are elongated for about 2.0º2θ. Example of stationary image close to 111 rlp is shown in Figure 3. The image has a periodic component as a maximum at 44.22º 2θ (2.046 Å) and a short range order component as a broad maximum at 43.604º 2θ (2.073Å).

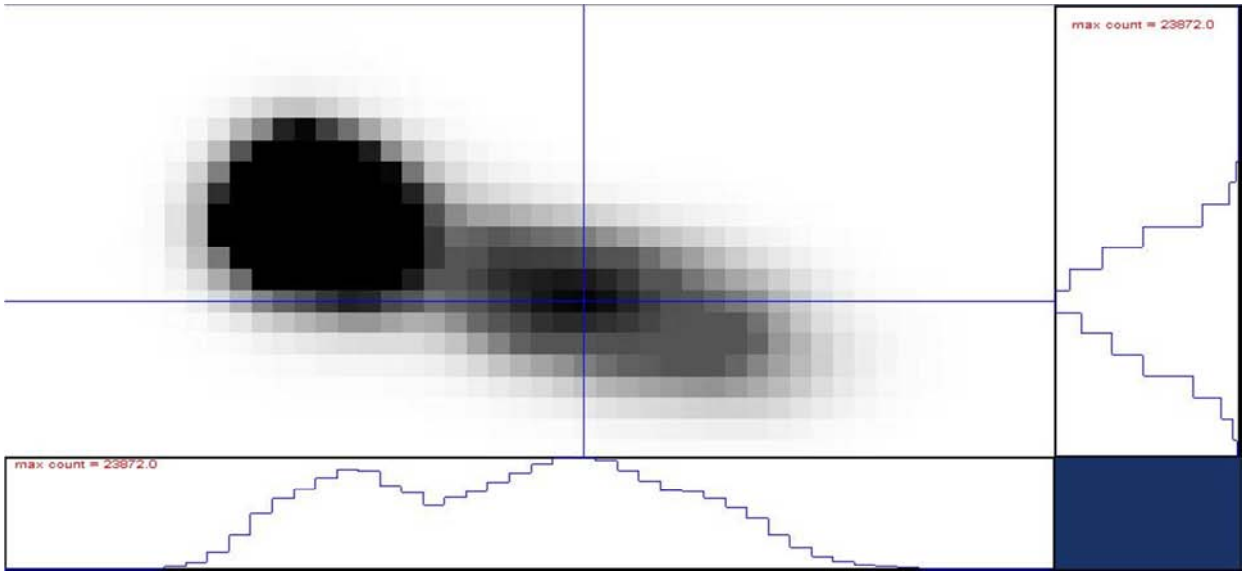

Figure 3. *Stationary diffraction spot as doublet from standard CVD crystal at the position close to strong 111 Bragg reflection at 44.22° 2θ /2.046 Å. The satellite of Bragg 111 reflection is at 43.60° 2θ /2.073 Å. The intensity ratio is 0.08 and the distance is 14 pixels.*

The discussion in [1] concluded that extra scattering should be assigned to static displacement of atoms from the lattice nodes. Again, we can divide scattering within the diffraction spot around 111 rlp into the long range and short range order components. The long range order maximum corresponds to lattice periodicity and is located close to 111θ of cubic diamond. Its FW0.5M is 6 or 7 pixels wide, which corresponds to 0.27 or 0.315º 2 θ. This maximum is in agreement with natural diamond FW0.5M of 0.31º 2θ The second, short range component exhibits scattering around the main 111 maximum: at high and low 2θ regions. The CVD reflections are broader than 111 reflections of natural diamond because of pronounced contribution of second component, as shown in Figure 1 and 2. Natural diamond spot extensions FW0.001M are in the range of 0.6 to 1.1º 2 θ depending on reflection. The extension of CVD reflections is typically around 1.5º 2 θ , in 1.0 to 1.75º 2θ range. Some 111 CVD reflections show broadening to such extent that the Bragg reflection and its satellites are not resolved. The other reflections appear as structural doublets which consist of a main maximum, located close to the position of 111 reflection of cubic diamond, and a smaller maximum. This smaller maximum is associated with the main one, because it appears during the same oscillation. For this reason we name them satellite reflections (Figure 1 and 2).

There are also more complicated distributions of intensity within the Bragg reflections. They can form triplets, i.e. 3 maxima are registered per reflection. The corresponding d_{111} values for standard crystal include:

Reflection #1: 44.26º (2.044Å), 44.04º (2.054Å), 43.76º (2.066Å),

Reflection #2: 44.22º (2.046Å), 43.81º (2.064Å), 43.57º (2.075Å),

Reflection #3: 44.28º (2.045Å), 44.11º (2.052Å), 43.69º (2.070Å).

These maxima show more preferences of specific interatomic distances within the wide distribution of atomic displacements.

The stationary reflection close to Bragg position from crystal A shows a triplet composed of strong maximum assigned to cubic diamond at 43.959º (2.057Å), and non-cubic features at 43.476º (2.078Å) medium intensity, and weak peak at 43.166º (2.093Å) (Figure 4).

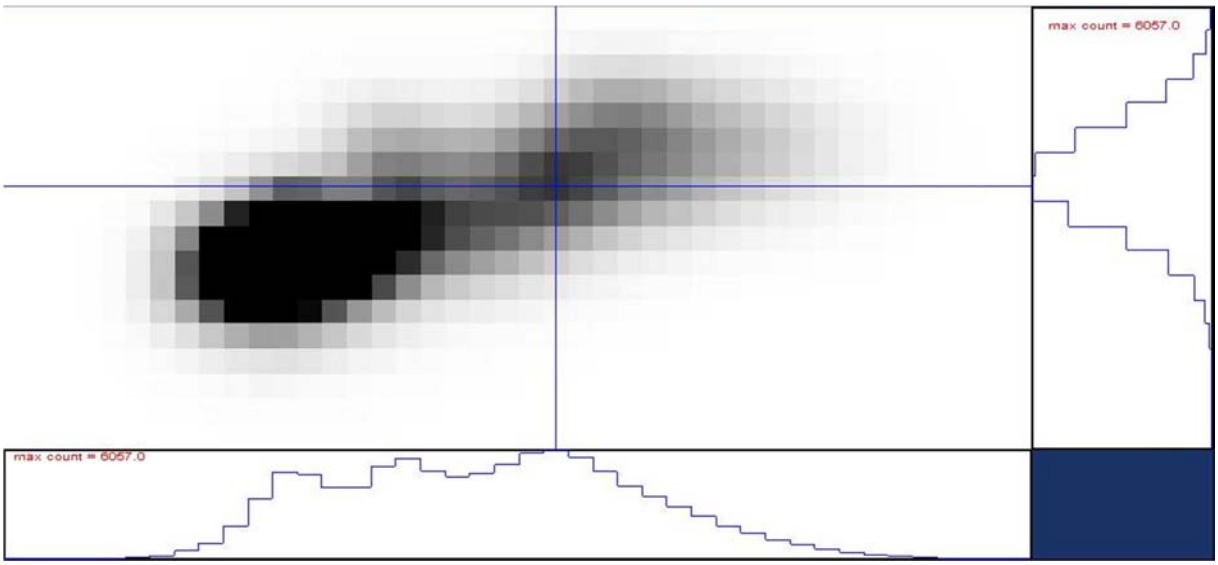

Figure 4. *Stationary diffraction spot as triplet from crystal A taken at the position close to 111 Bragg reflection. Three maxima are within the spot. The Bragg position is close to 43.95° 2θ/ 2.057 Å. Satellites are at 43.47° 2θ /2.078 Å and 43.16° 2θ/ 2.093 Å.*

Satellite reflections on both sides of Bragg positions appear as a rule for ω shifts from 111 rlp's for three studied crystals. The stationary spot at $\Delta\omega = 0.25°$ from the standard crystal appears as doublet of reflections on both sides of Bragg positions. The stronger maximum is at 43.44 2θ (2.080Å), and the weaker one is at 44.77 2θ, (2.022Å) (Figure 5). For the shift equal to 0.5^0 ω , the stronger maximum is at 45.14º 2θ, (2.01Å), and the weaker reflection at 111 diamond position is at 43.87º. The width of the" rocking curve" was 1.5º ω at the base for crystals A and standard. In comparison, the "rocking curve" width for natural diamond is 1.0ºω.

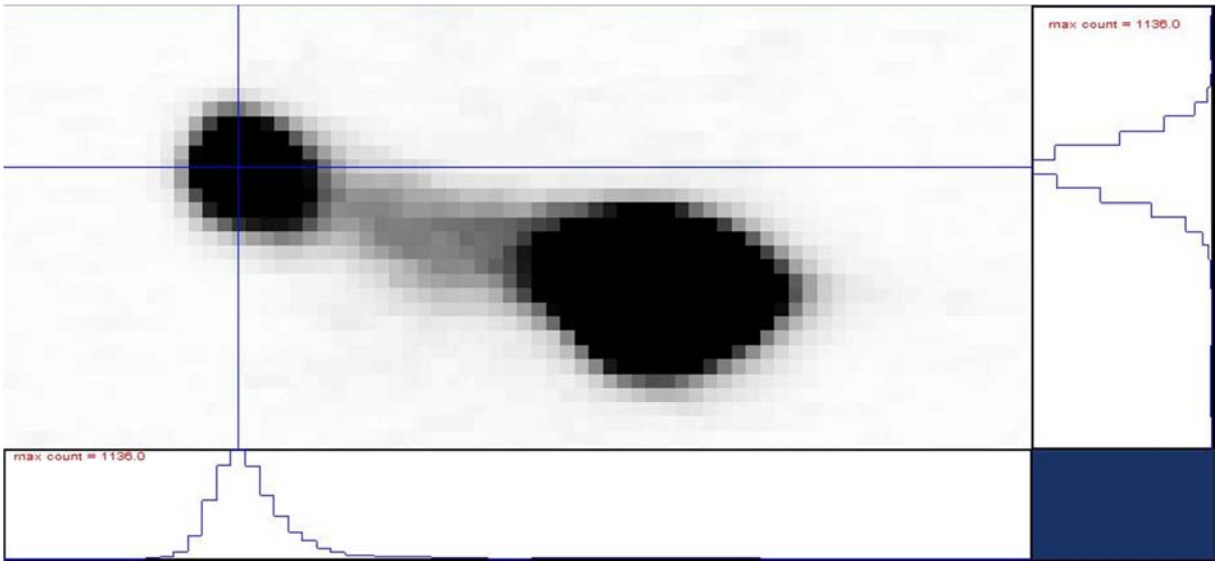

Figure 5. *Satellites for stationary standard CVD crystal shifted for 0.25ºω from 111 Bragg position. Satellites are located outside of the position Bragg reflection, on smaller (43.44 ° 2θ /2.080 Å) and larger (44.770 ° 2θ /2.022 Å) angles, as shown in profile.*

In summary, the displacement disorder of atoms in CVD single crystals is attributed to the two types of scattering around 111 rlp. The directly observed scattering beyond profile of natural diamond corresponds to atomic shifts larger than the ones existing in natural crystal. The second type of scattering is the anomaly in the shape of Bragg reflection, which is observed as structural doublets and triplets. They constitute a unique feature for cubic diamond crystals grown in the presence of nitrogen. The doublets and triplets, not reported previously, indicate the presence of specific interatomic distance of atomic pairs that are not observed for cubic diamond. The distribution of interatomic distances is a complicated 3-dimensional function because of anisotropy of scattering around rlp in reciprocal space. The rounded shape of satellites reflections does not indicate planar defects. They correspond to rounded cross-section of X-ray beam passed by collimator.

220 Rlp (12 Planes)

There are 12 equivalent {220} planes for diamond point

symmetry group. The data from three CVD crystals are consistent with respect to the 2 classes of 220 reflections: broad and resolving spectral doublet. The calculated resolution of CuKα1/α2 spectral doublet is 0.218º 2θ. The broad reflections are asymmetrical with tail toward the smaller θ, for example peak width FW0.5M = 0.45º2 θ (Figure 6). Peak maximum in Figure 6 is located at 75.221º 2θ. Calculated, using diamond lattice parameter, value of 2θ for CuK α_1 is 75.277º 2 θ (d_{220} = 1.261Å and interatomic distance 1.544Å). Spot extension at FW0.001M is 2.98º2θ. Edge of the spot at 76.150º 2θ corresponds to d_{220} = 1.249Å, and interatomic distance in tetrahedron is 1.525Å. The edge of the spot at 73.171º 2θ corresponds to d_{220} = 1.292Å and 1.578Å interatomic distance in tetrahedron. These are the estimated values, which can be assigned to maximal displacements of atoms from lattice nodes according to 220 reflection. The full range of atomic shifts, on both sides, is 3% of inter-atomic distance.

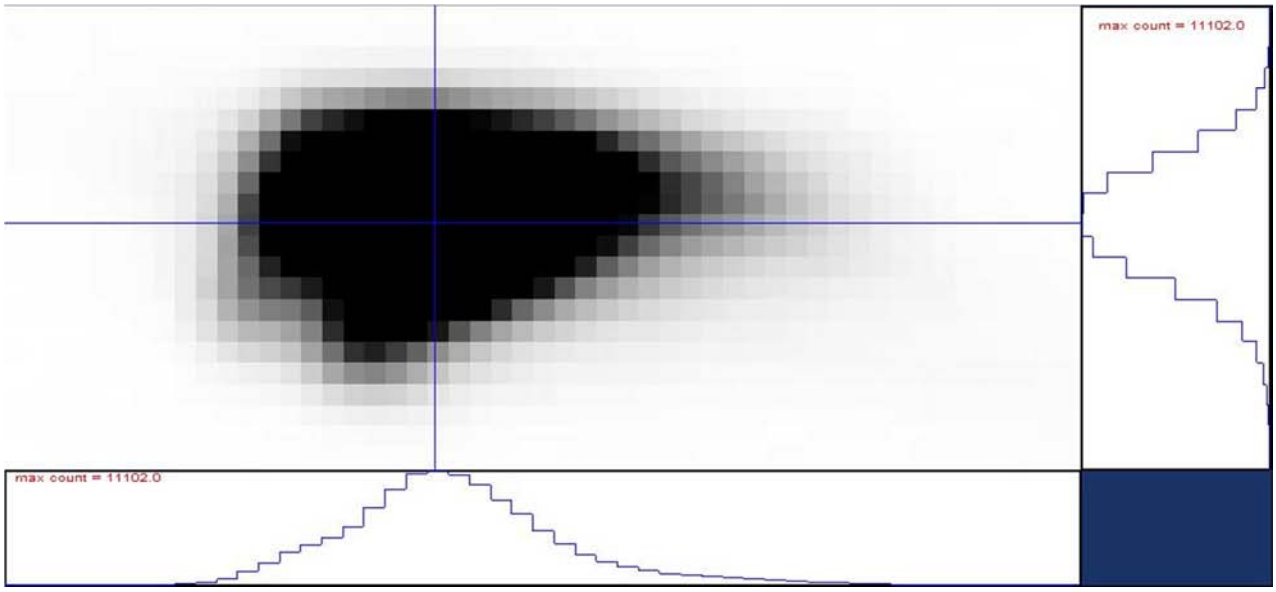

Figure 6. *Oscillation (within 10°ω) image of 220 reflection from crystal A. One wide spot has maximum at 75.220° 2θ / 1.262 Å, FW 0.5 M= 0.27° 2θ, the width at spot edges ≈ 3° 2θ.*

Stationary reflection was registered at 1.5º ω shift towards smaller angles from 220 Bragg position. The reflection has triplet form. The main maximum is at 73.846º (1.282Å), and maxima on both sides are at 74.269º 2θ (1.275Å) and 73.515º 2θ (1.287Å). For the last one, the shift from lattice node is 2%. The edges of the spot are at 73.24º and 74.81º 2θ. These edges are outside the natural diamond spot shown in Figure 3 in reference [1]. The maxima within stationary spot in Figure 7 cannot be assigned to spectral doublet. They are related to short range order of atoms, and they show the preference of correlations of pair of atoms in specific crystallographic direction.

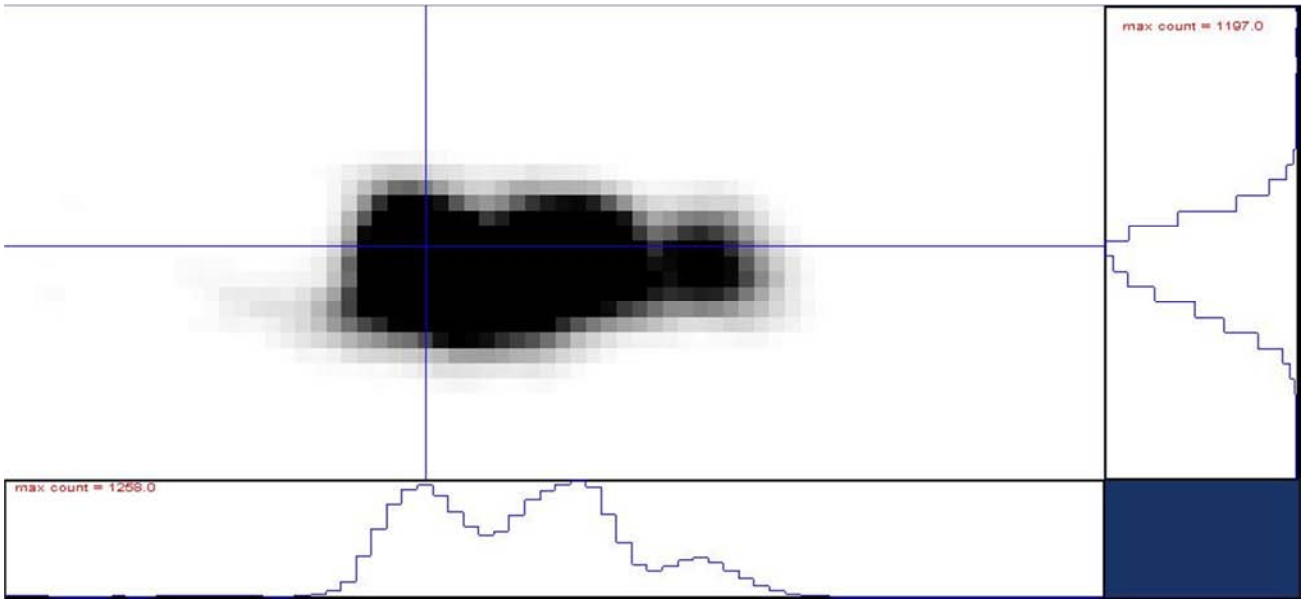

Figure 7. *Stationary triplet image of 220 reflection from crystal A. The maxima are at 73.51° 2θ /1.287 Å, 73.846° 2θ /1.282 Å and 74.268° 2θ /1.275 Å.*

The narrow 220 reflections that exist have FW0.5M = 0.22º 2θ; however they have weak spectral resolution. The extension of reflections FW0.01M is around 1º 2θ. In summary, the short order component has a pronounced contribution to some 220 reflections. In addition, a strong anisotropy exists among 220 reflections. Some of these reflections show significant shifts of atoms, whereas the other ones indicate the smaller displacements.

311 Rlp (24 Planes)

Calculated d_{311} = 1.0755 Å. 2θ for Kα1 is equal to 91.484º, and 91.775º for Kα2. So spectral resolution is 0.291º 2θ. We can divide 11 reflections recorded for CVD crystals into two groups. One group shows limited spectral doublet resolution. One such reflection is shown in Figure 8. The main maximum is at 91.708º, and can be assigned to Kα1. Second maximum at 92.004º is attributed to Kα2. Weak maximum at 91.512º, is a non-cubic feature. Other 311 spots have extended tails just in this place. These tails toward smaller θ indicate the existence of atomic pairs with larger interatomic distance compared diamond unit cell. The spots extension at the base of reflection is around 1.2º 2θ. The second group of 311 reflections consists of broaden reflections. They show no spectral resolution, and have tails toward small θ. FW0.5M is 0.35º 2θ, FW0.01M = 1.6º, FW0.001M = 2.7º.

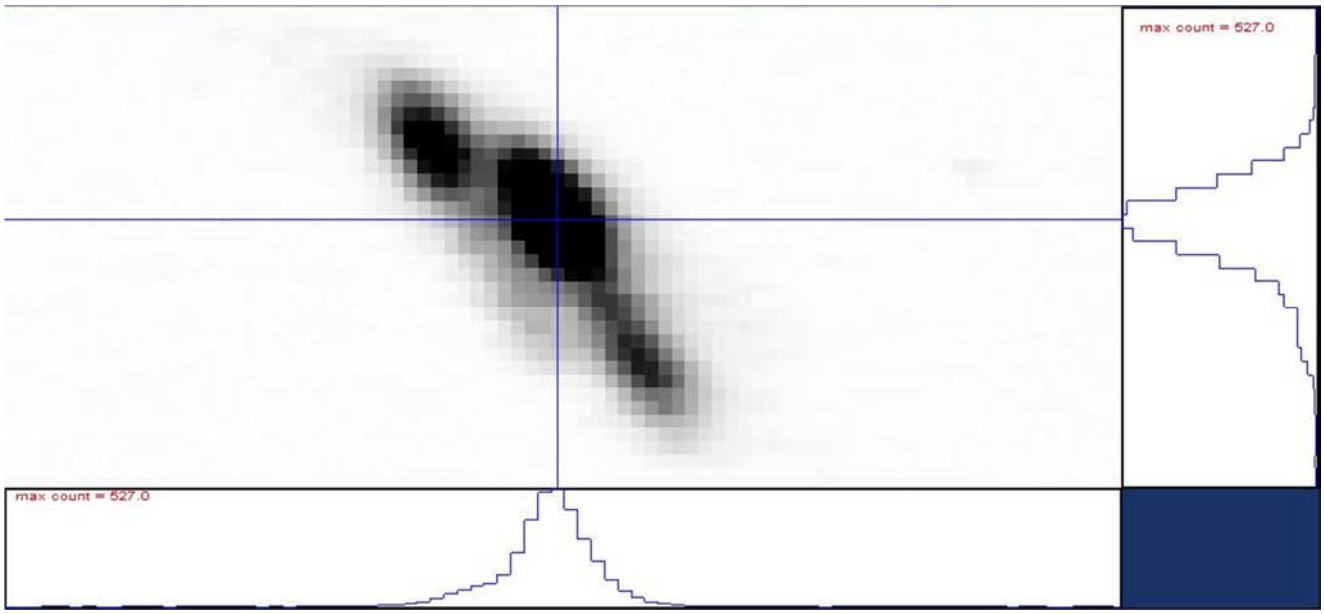

Figure 8. *Oscillation (within 3° ω) image of 311 reflection from standard CVD crystal. The central peak at 91.708° 2θ /1.073 Å maximum of 311 reflection and larger θ maximum at 92.00° 2θ corresponds to Kα2 maximum. The third maximum constitutes a satellite at 91.57° 2θ /1.070 Å.*

222 Rlp (8 Planes)

These are forbidden reflections for cubic diamond space group.. For CVD crystals, the measured maximum peak intensity ratio of 222 reflection to 111 reflection is 0.04, 0.025, 0.04 for A crystal, standard crystal and plate respectively. In comparison, the ratio for natural crystal is 0.01 [1]. We speculate that CVD crystals differ from natural crystals in static defects. These defects can introduce changes in distribution of electron density in unit cell of diamond and in consequence to the intensity of Bragg reflections. Some specific static defects configuration should be suggested, which alters electron density distribution proper to diamond chemical bonding. This can be the reason for the increase of above ratios.

The oscillation images are shown in Figure 9 and 10. The calculated spectral doublet resolution is 0.32º 2 θ and corresponds to between 7 - 8 pixels. Figure 9 shows oscillation image of 222 spot from standard crystal. The observed and calculated $Kα_1$ maximum is at 96.990º and at 96.828º 2 θ, respectively. Similarly, for Kα2 maximum observed and calculated is at 97.301º and 97.146º, respectively. Figure 10 shows spectral doublet for crystal A which is more irregular in shape, but the maxima fell close to calculated, 96.802º and 97.204º 2θ, respectively.

The observed maxima correspond to periodic part of intensity function. Short range order contribution is small.

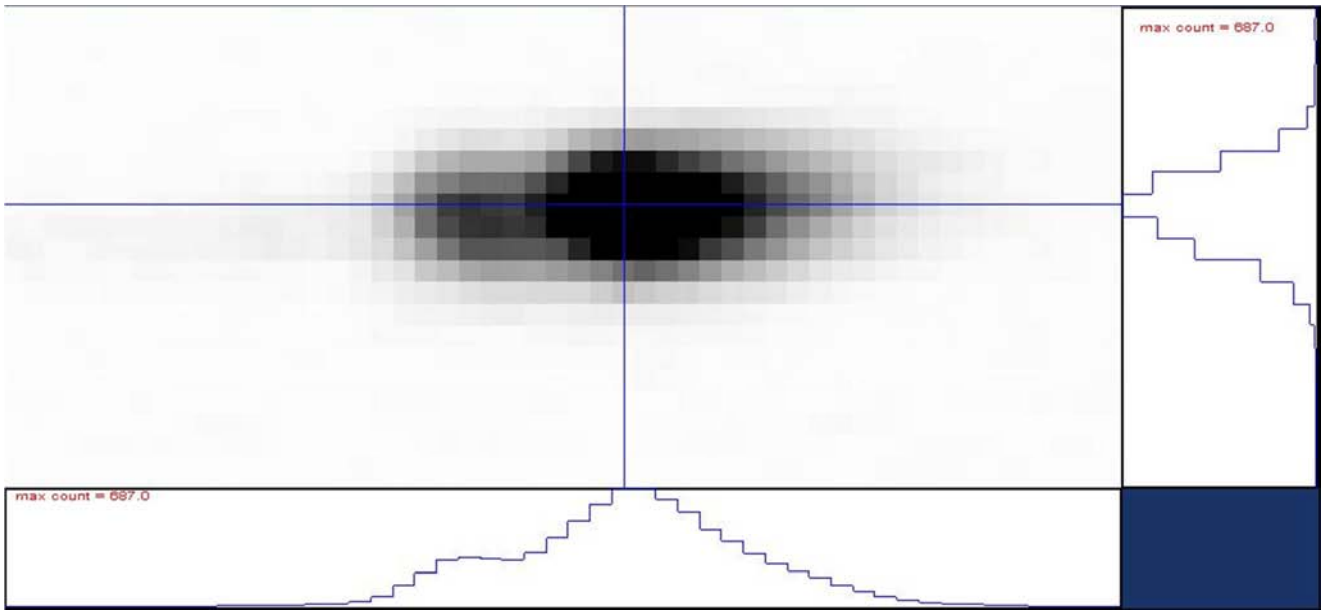

Figure 9. *Oscillation (within 2°ω) 222 reflection from standard CVD crystal. The main maximum at 97.000° 2θ /1.028Å corresponds to Kα1, and second one at 97.301 corresponds to Kα2. Long tail runs towered larger θ, not shown.*

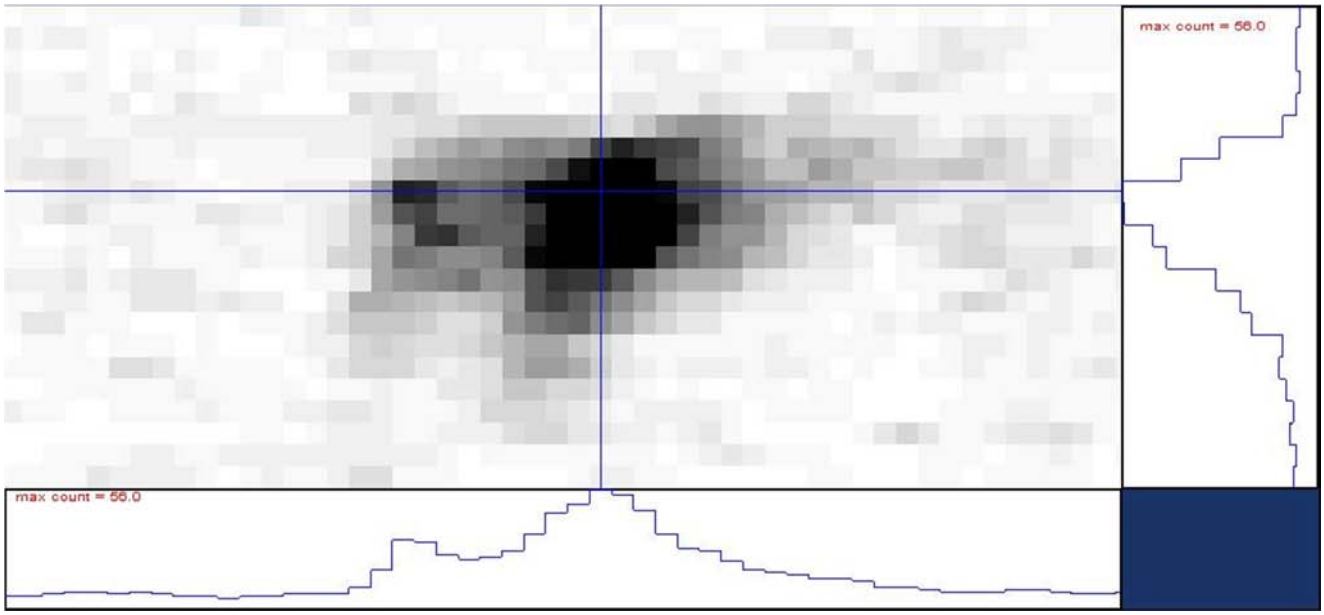

Figure 10. *Oscillation (10° ω) image of 222 reflection from crystal A. It looks like spectral doublet. Maxima are at 96.802° 2θ /1.030 Å and 97.204 ° 2θ for Kα2.*

400 Rlp (6 Planes)

The 4 independent reflections were studied. The spectral doublet was clearly resolved in CVD crystals at 0.486º 2θ. The FW0.5M for $K\alpha_1$ component maximum is 0.22º 2θ, which is less than for natural diamond values of 0.36^0 and 0.26º for reflection of Si located close to 222 diamond. One strong stationary $K\alpha_1$ 400 reflection was sharp with FW0.5M equal to 0.18º 2θ. Long range order part was dominant in this case. "Rocking curve" build from the consecutive stationary images for $K\alpha 1/\alpha 2$ spectral components has FW0.5M = 0.5ºω wide. At the base the curve extends to 1.7 º ω. There is difference in sharpness among other 400 CVD reflections.

331 Rlp (24 Planes)

331 reflections are relatively less disturbed, which indicates that contribution from short range order is negligible. They represent long range order component of CVD crystal lattice. The spectral doublet is well resolved, and is close to the calculated 0.795º 2θ resolution. The d_{331} calculated for λ Cu $K\alpha_1$ is 0.8183Å, which is close to measured values for natural diamond (0.8178 ±0.0002 Å) and CVD crystals (0.8179 ± 0.0002 Å). Therefore, conclusion is that lattice parameters fall close together, indicating that θ measurements are consistent for all hkl. The error is calculated based on the assumption that the uncertainty of 2θ is 1 pixel, which is equal to 0.045º 2θ. CVD lattice parameter corresponds exactly to natural diamond.

The sharp profile of 331 line, located on high θ angles, indicates on long range order component in CVD crystal.

3.2. Summary on X-Ray Diffraction: Short and Long Range Order Combination

Based on general discussion of x-ray diffraction from disordered structures in [1] and obtained experimental data in the present report, a combination of short and long range order is suggested as the main feature of atomic structure of CVD single crystals grown with N_2 participation. CVD diamonds crystal structure relates to order-disorder issue.

The existence of scattering in the vicinity of rlp's indicates static displacement of atoms from the nodes of periodic cubic diamond lattice. This scattering is related to the short range order, and is more pronounced around 111 and 220 reflections, while less pronounced scattering is around 311. Some 400 Bragg reflection profiles are sharper, than for natural crystal which suggests that 400 scattering is almost solely related to the long range order. Similarly, the 331 reflections profiles are close to the periodic part of atomic distribution in natural diamond crystal.

This behavior of x-ray intensity at sequential reflections as function of 2θ indicates short range order connection to the extra scattering around 111, 220 and 311 rlp. This scattering corresponds to atomic pair correlation within defect field. The interatomic distances in these pairs differ from the distance in diamond unit cell. We recall the function of atomic pairs correlation calculated for amorphous materials as an analogy to the case under consideration. The scattering from such materials appears in this particular region of reciprocal space.

X-ray diffraction confirms clearly the existence of periodic matrix as in natural diamond, on which the displacement of carbon atoms, resulted from static defects, is superimposed. The displacements reach up to 2%, or more, of interatomic distances. The distribution of interatomic distances is a complicated function in the shift in vector space of autocorrelation function. X-ray diffraction, in our case, is not able to provide directly the geometry of atomic configuration(s) of growth defect. The geometry of static defect which imposes shifts of atoms around it, is an area for future investigation. The existence of static defects was deduced from broadening and satellites.

3.3. Raman and Luminescence Spectroscopy

Raman spectra from (001) CVD single crystals fit well to the spectrum from nearly perfect natural diamond crystal. By the same token, Raman spectra confirmed good crystallographic quality of studied single crystals. The spectra were taken on the top surfaces of plates and gemstones and show only the main peak of cubic diamond at 1332 cm^{-1} and low background at 1500 cm^{-1} region. One plate crystal had a few inclusions which appeared on the top surface during growth. Fortunately, they helped to understand the origin of mysterious 1500 cm^{-1} band. The inclusions to single crystal were seen as less than 1 mm in diameter hemispheres grown on the surface.

X-ray diffraction taken from one such hemisphere produced so called "powder pattern" of cubic diamond, i.e. polycrystalline material with randomly oriented cubic diamond grains. On the top surface there are two types of facets: squares and tringles. This means the inclusion is made of crystal grains grown by two different mechanisms. One like epitaxial growth around the inclusion, namely (001), seen as squares and the second ones of symmetry along <111> growth. This second growth appears during (001) growth as disturbance because of <111> twin formation.

Raman spectrometer allows focusing laser beam just on such individual micro facets, few microns across. Spectrum from square facet resembles the spectrum from the neighbor surface of single crystal. Spectrum from triangular facet is different; it belongs to <111> growth sector. It has the 1332 cm^{-1} peak and a broad maximum around 1500 cm^{-1}.

This is a crucial point for the explanation of the origin of wide 1500 cm^{-1} band. The band appears for <111> growth sector. The epitaxial growth on (001) and growth of <111> crystal grains in inclusion proceed under the same process parameters and at the same location in plasma. The <111> twins are originated on (001) surface and continue to grow as inclusion. Around the inclusion epitaxial growth runs undisturbed, so we predict there should be no graphitic phase also in twined part of inclusion. The main structural feature of this sector, grown in the presence of nitrogen, are (111) stacking faults. They are arranged randomly, creating planar disorder. The planar disorder was caught with electron diffraction and x-ray diffraction patterns as described in [1], where the concept of sp^2 bonding as the cause of 1500 cm^{-1} band was rejected due to lack of factual support.

From the point of view of single crystal structure of cubic diamond, x-ray diffraction patterns of material grown inside <001> growth sector and inside <111> growth sector are distinctly different. In other words, <001> epitaxy produces materials of different growth defects. Below are the examples of x-ray diffraction patterns received for <111> growth.

The planar disorder was clearly demonstrated earlier in <111> epitaxy. Epitaxial growth on (111) as- grown face of natural octahedral crystal at 900°C, 1% CH_4 in H_2 yielded a highly oriented (111) film, 100 μm thick [12, 14]. X-ray diffraction stationary pattern from 111 reflection region is shown on photographic film in Figure 11. The pattern was taken in Debye-Scherrer camera, 114 mm in diameter. We see longer arc of 111 Bragg reflection of cubic diamond at 2.06 Å and shorter, wider arc of satellite reflection at 2.12 Å. The left side of image corresponds to smaller θ angles. The satellite reflection can come from mixed cubic – hexagonal stacking. Diffuse scattering is composed from 3 streaks and a spot. Streaks correspond to planar defects; in this case, to stacking faults, and spot on higher θ angles to linear defect as shown in Figure 11.

Creation of diamond ordered polytype was demonstrated during epitaxial growth on (001) square plate of High Pressure/High Temperature (HP/HT) single crystal diamond of Sumitomo Co. The sides of this plate were cut along (100) plane and equivalent, in contrast to plates studied in this

project, cut along (110). The growth process was conducted in similar conditions as for (111) epitaxy above. X-ray diffraction was taken at the corner of the plate by rotation crystal method. We can expect following growth sectors in this place: 111, 001, 100 and 010. The crystal was rotated around <001> axis. The diffraction pattern is composed from Bragg reflections of cubic diamond, and forbidden reflections. The forbidden Bragg reflections were assigned to diamond polytype. The super-structure reflections have positions on sub-levels, which are in the distances at 1/3 and 2/3 between equatorial and first level of cubic diamond. The super-structure reflections correspond to triple periodicity of cubic diamond. The triple periodicity can impose 111 layers sequence as a mixture of cubic and hexagonal stacking of this ordered polytype. [12, 13]

These independent growth experiments indicate creation of stacking faults in growth environment similar to conditions of (001) epitaxy, leading to conclusion about direct relation of stacking faults to 1500 cm^{-1} band in Raman spectra. This is also manifestation that single crystal cubic diamond cannot be grown on (111) face substrate during CVD microwave plasma process.

Raman and luminescence spectrum from 100 μm film, which x-ray diffraction is shown in Figure 11, was measured with green laser (514 nm) contains 1335 cm^{-1}cubic diamond line and much stronger broad band with maximum at 1485 cm^{-1}. The spectrum taken with blue laser (488 nm) looks similar except the second maximum is shifted to 1443 cm^{-1}. This shift is difficult to explain. The details of 1500 cm^{-1} band differs between CVD materials. For example, film grown under plasma ball, as described in [9] showed relatively sharp maxima at 1552 (green laser) and at 1548 (blue laser).

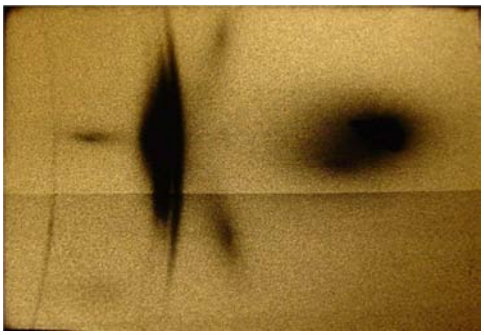

Figure 11. *X-ray diffuse scattering around 111 rlp, registered on photographic film with Cu radiation, filtered by Ni foil in 114 mm diameter Debye-Scherrer camera. The diffraction comes from epitaxial diamond film grown on 111 face of natural diamond. There is a sharp arc for 111 reflection of cubic diamond at 2.06Å, and a shorter wide satellite arc, at 2.12Å. 3 streaks correspond to planar defects and large spot for linear defect. The diffuse spot partly overlap Laue spot. Smaller θ are on the left side.*

Returning to CVD gem crystals grown with N addition, luminescence spectra, which accompany Raman spectrum, were measured in the range of 2000 – 6000 $cm^{-1.}$ A series of peaks is superimposed upon the broad hump. Usually a combination of impurity atom(s) and growth defect is responsible for rising luminescence. Some gem crystals showed relatively low level of luminescence, which is a significant observation.

3.4. Description of <110> Linear Defect Hypothesis

Previous study of growth sectors in CVD crystals indicated that crystallographic perfection of the <001> sector is high, and <111> sector is disturbed by planar defects of high density [12]. For different growth sectors growth mechanisms are different despite of the same growth environment.

This report seeks explanation of IDP images for CVD crystals, which show a drastic change of x-ray scattering in the vicinity of rlps compared to the images from natural diamond and Si. The satellites present there show that some atoms are shifted up to 2% of interatomic distance of C atoms in diamond lattice, which is a direct proof for the defects in diamond lattice. The next fact is a pattern of parallel lines <110> on the fractured surface (110). Unexplained are <110> single rows between dimers rows on (001) reconstructed surface observed with Scanning Tunneling Microscopy (STM) images. The arms of <110>/<1-10> cross observed inside single crystal plate with the naked eye also show the linear nature. All these experimental facts point toward the existence of linear defects. But what is the real cause of static displacement of atoms there? Exact description of growth defects requires the knowledge of atomic configuration, which disturbs periodicity of crystal matrix, and the knowledge whether foreign atoms are present in this area. According to x-ray diffraction, part of tetrahedra in diamond lattice is deformed. However, to describe the deformation in the case of complicated anisotropy of x-ray diffraction spots from CVD diamond crystals, grown with nitrogen addition, is a challenging task.

We are expecting help from high-resolution TEM imaging in determination of geometry of atomic configuration of local lattice defects. The present aberration-corrected high-resolution TEM imaging techniques can demonstrate atomic resolution in images of diamond lattice. The study on planar defects [15] clearly states: " For the first time, diamond in in <110> zone –axis orientation was imaged in STEM mode at a resolution that allows for resolving the atomic dumbbells of carbon at a projected distance of 0.89 Å." Twin boundaries revealed local atomic distortions which break the symmetry of the ideal boundary and more importantly voids on the atomic level were observed.

These results are supportive in the case of linear twin hypothesis, however it would be more conclusive having x-ray and HRTEM images just from the same sample, i.e. (001) homoepitaxial growth in the presence of N_2. Unfortunately such images have not been published, so we have no direct insight. Linear twin hypothesis is based on available experimental data and theoretical considerations. One such hypothesis was described in previous paper on oriented diamond growth on (001) Si, where the influence of presence of N_2 on growth process is possible [16]. Now we elaborate this concept in more detail.

At this point we recall previous study on (001) homoepitaxy using microwave plasma CVD process. [12]

The experiments were conducted in a tubular system using mechanical vacuum pump, so the base pressure was around

10^{-3} Torr. It also happened, that small air leak sometimes took place. In such situation diamond growth proceeded under low concentration of N and O.

When broken along <110> line, the homoepitaxial diamond film, grown on (001) natural diamond substrate, shows different cleavage for the film and for the substrate. The CVD film cleaves along the (110) plane, whereas the natural diamond crystal typically cleaves along (111) plane. This demonstrates the important difference between these crystals from the point of view of lattice defects, and this fact is used as a starting premise in consideration of new (001) growth defect in diamond CVD film. Cleavage surface is characteristic because of the set of parallel lines running in <110> direction. SEM images stay similar despite increasing magnification. The density of these lines is high. The distance between them falls below 0.2 μm [12]. Similar pattern of lines was seen in cleaved single crystal plate, 2 mm thick, studied in this project.

These lines may have a connection to CVD growth defect. The consideration now will follow the linear nature of this growth defect, and the growth mechanism on (001) diamond surface. During step growth on slightly inclined surface of diamond substrate, when terraces are formed, foreign atoms (like H, N and some complexes) participate in the process of adsorption of radicals and abstraction of H. We suspect that mistakes created during H abstraction process from methyl radicals, attached to the surface, caused some H atoms to remain incorporated into the lattice. Incorporation of N atoms is probably one order of magnitude less and the role of N species in enhancing (001) growth rate is still unclear.

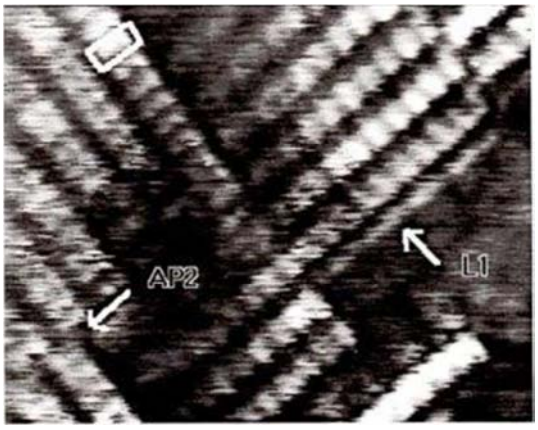

Figure 12. *High-resolution STM image of (001) hydrogenated surface of homoepitaxial CVD diamond film to show dimer-type 2x1 reconstruction. Some individual dimers are resolved as one in the box. AP2 represent antiphase boundary. L1 represent a single row, presumably related to a linear twin in <110> direction. The scan area is approximately 58x44 Å. Courtesy Yalei Kuang PhD Thesis 1997 PSU.*

The insight into step growth was possible due to scanning tunneling microscopy (STM) study of homoepitaxial films conducted earlier [16 - 21]. STM images are produced when studied surface is electrically conductive. Diamond was lightly doped with boron. The important step in preparation of diamond surface for STM study requires etching in microwave hydrogen plasma. During last minutes of growth process, the top atomic layers of deposit are disturbed. Etching with atomic H removes these disturbed layers on the crystal surface and exposes inner crystal planes for study. After etching, the top surface is hydrogenated, i.e. H atoms are chemically bonded to carbon atoms underneath. Such hydrogenated surface is electrically conductive [22]. STM images show distribution of H atoms on a diamond surface. Hydrogenated surface is reconstructed and dimers on terraces are observed as double rows. The positions of C atoms can be anticipated from dimers orientation. Dimers rows do not reflect exactly the symmetry of diamond lattice underneath. Figure 12 shows an image of resolved dimers rows. There are images of two H atoms which are 2.5 Å apart, shown in the box. Atomic resolution is achieved here. This unique image was obtained by Yalej Kuang [18].

In Figure 13 the resolution is lower, and dimers on terraces resemble hand fingers. There are areas where fingers are arranged regularly. So that C atoms formed periodic lattice underneath. On such surface the growth proceeds. The growth defects can be created because of the presence of hydrogen and nitrogen atoms, molecules, radicals and binary and ternary C-N-H species. The sequence of fingers is disturbed. It looks like a stripe between fingers. The stripes, once defect is generated, continue to be observed in <1-10> direction. The neighbor dimer rows are undisturbed. It means that anticipated growth defects, seen in Figure 12 and 13 as single rows run in <1-10> direction and are narrower than dimer rows, which have 5Å width. The dimer – single row system is named as a local 3x1 configuration. In the case of Si 3x1 configuration consists of periodic set of 3x1. The periodic set was not observed on diamond. At this image resolution, no structure of the stripe (single row) is shown [20]. Single rows were also reported in reference [23]. The STM study was conducted on (001) surface of homoepitaxial films grown by hot-filament method.

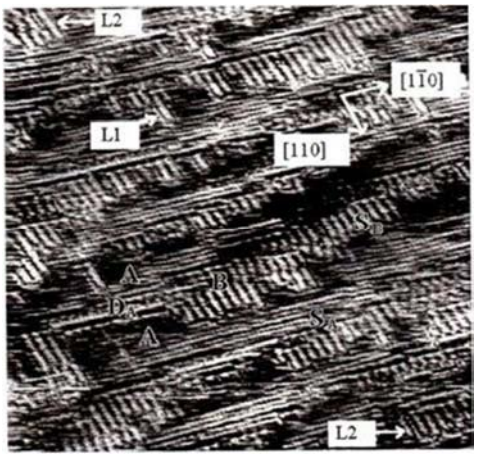

Figure 13. *Large-area STM image of (001) surface of CVD diamond film shows the 2x1 and 1x2 double domain surface structure. The substrate was misoriented by 1.3° and 0.7° toward <110> and <011> directions. Two type of terraces and single-layer step are labeled B, SA, and SB, respectively. A double-layer step running parallel to dimer rows is labeled DA. Single rows are marked L1 and L2. Together we see more than 10 single lines in the image. The area is approximately 200x350 Å. Courtesy Naesung Lee, PhD Thesis, 1996 PSU.*

It is possible that a linear growth defect is hidden under the surface of single row. No higher magnification was achieved, no experimental evidence on how atoms are located along such line. The single row is approximately 2 times narrower from dimer. The single row-dimer system has a critical meaning in reasoning about linear defect. The orthogonal dimer patterns confirm step growth mechanism for CVD (001) diamond and disturbances of it are observed. This important experimental finding cannot be neglected and it correlates with the cross, observed with a naked eye, as bundles of <110> and <-110> lines. This relates to micro-macro correlation.

The founder of crystallography, Rene Just Haüy (1773 - 1822), suggested a macro to micro correlation in crystals. Rhombohedral calcite crystal easily brakes to rhombohedral pieces (macro) when falls on ground. He deduced that this crystal is built from the very small rhombohedral elements (micro). These elements are unit cells in the periodic lattice. Crystallography and solid state physics disciplines were originated from this simple concept. As an analogy, the threads constituting bunches of the cross arms and seen by the naked eye (macro), can be related to the single rows of STM images (micro) and also lines on a fractured surface in SEM images.

The regular dimer patterns appearance suggests that the perfect diamond lattice can be expected underneath. The distance between dimer rows is 5.0 Å. The length of single rows is 20-50Å on presented STM images. The other part of single row is hidden under the top terrace. Observation of these rows is limited to the length of terraces. It can be suggested, that a single row marked with letter L in Figure. 12 and 13, corresponds to hydrogen atoms adsorbed along the defect line <110>, which runs on the (001) surface and was exposed to etching with atomic H.

Below the very surface of H atoms, along the single row, the atomic configuration is expected to be different than in diamond unit cell. Such configuration does not produce dimer on the top surface. The atomic configuration of defect itself, which goes along <110> line, is anticipated in Figure 14. The justification for this configuration is in the geometry of specifically oriented tetrahedra in diamond unit cell.

Presently only <111> type of twinning is considered. It is a dominant characteristic of diamond [24]. It takes place along <111> axis. On (111) plane two parts of crystal lattice has mirror reflection. This twinning is seen in macroscopic and microscopic images, as well as in high resolution TEM images. It reorients tetrahedra, but structure preserves connection of tetrahedra at corners. It produces planar disorder, and in consequence atomic displacements.

Now new atomic configuration can be considered during (001) homoepitaxy, because x-ray scattering around rlp's is different than for <111> growth. It is not fully recognized yet, however, defect lines are real. Single rows seen in Figure. 12 and 13 are the critical objects in consideration of this hypothesis, so that (001) linear twin is formed by mirror reflection in (001) plane, which makes the line of tetrahedra in <110> direction to share the edges as result of addition of atoms during the row building (Figure 14)

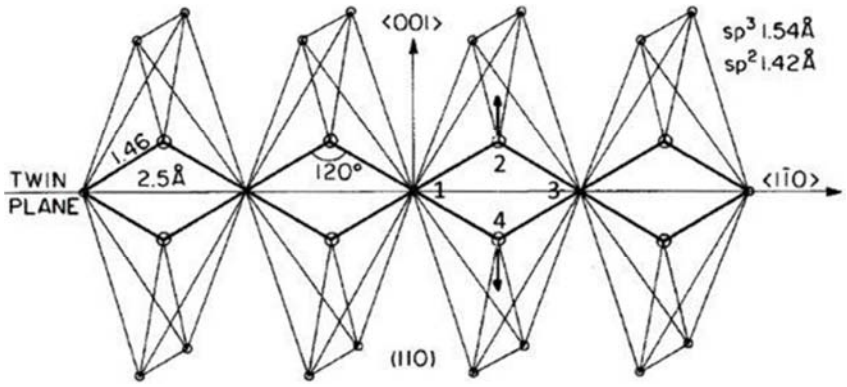

Figure 14. *Row of tetrahedra sharing edges along <1-10> direction on the left side of <001> axis; no deformation of tetrahedra. On the right side arrows, drawing indicate shift of atoms #2 and #4 to fit diffraction data.*

The model of <110> linear configuration is built upon the twinned tetrahedra, which share edges, in contrast to cubic diamond structure where tetrahedra are connected at the corners. Despite the fact that twined two rows of tetrahedra do not change the number of carbon atoms in the modified unit cell, the model introduces a strain within the tetrahedra. In this model we have (111) facet and (11-1) facet create the twin as reflection in the mirror of (001) plane. It correlates with the image of the real fractured (110) surface, which is composed of micro-facets (111) and (11-1) described above on the basis of SEM image. It also correlates with epitaxial growth on (110) substrate, where instead of (110) atomic surface, long micro-facets (111) and (11-1) appears as a rough surface. This is inconvenient truth about <110> growth [12].

The model of linear <110> defect considers the local change of diamond structure, where a shift of tetrahedra according to twin on (001) plane is suggested, as shown in Figure 4 of paper [16] and in Figure.14. The shift of atoms causes a significant tetrahedral coordination disturbance, because it changes the order of filling octants in diamond unit cell. Atoms #2 and #4 have a 5-fold coordination, according to such configuration. It cannot be like this. H atoms are expected to substitute some C atoms. The incorporation of H atoms along this line will balance bonding equilibrium of C atoms. We imagine linear defect as a tunnel along <110>,

filed with C and H atoms and mixed with vacancies. The diameter of such tunnel can be 5 Å. Atoms in such tunnel can adjust their positons to satisfy condition of chemical bonding equilibrium with surrounding lattice of cubic diamond. This configuration is persuaded of because the appearance of x-ray diffraction satellites of Bragg reflections, STM single rows, SEM lines of cleavage and H atoms incorporation up to 1000 ppm, and independently observed in IR spectra [13].

The cross-section of hypothetical, twinned atomic configuration is shown in Figure.14. The plane of drawing is parallel to (110). The left part of drawing shows carbon atoms at the positions of regular tetrahedra from cubic diamond lattice. Along <1-10> direction a sequence of rhombi is formed. The interatomic distances in rhombi are equal to 1.46 Å. This value falls in between 1.54Å for diamond and 1.42Å for graphite. This configuration on the left side, which should produce a single satellite corresponding to 1.46 Å, does not fit to the situation observed with 111 Bragg reflection satellites, where satellites correspond to interatomic distances larger and smaller than 1.54 Å. With the modification of configuration described in [16] one can fits the new x-ray diffraction data. The satellites appear during oscillation of diamond crystal across the Bragg position within a small ω range. We are allowed to use Bragg equation to calculate d value for satellites within this range, and obtain interatomic distances for satellites which originate from the shift of atoms within this configuration.

The 111 satellite located on smaller θ angles, than Bragg position, has d value around 2.10 Å, comparing to 2.058Å for 111 of diamond. Also interatomic distance will be larger, namely 1,57 Å, so atomic shift is close to 2% of interatomic distance in tetrahedron. The satellite located on larger θ angle has d value of 2.02 Å and corresponds to interatomic distance of 1.51 Å. Atomic pair contraction is about 2%. Combining these data we have wide Bragg reflection, which corresponds to the wide distribution of interatomic distances, where we have 3 maxima. The main maximum expresses domination of 1.54 Å interatomic distances as in cubic diamond. On the both sides of 1.54 Å there is continuous distribution of interatomic distances with maximum at 1.57 A, and weaker maximum at 1.51 Å. This distribution reflects displacement disorder of atoms around the defect line; we have longer and shorter inter-atomic distances than in cubic diamond.

The assignment of satellites to shift of atoms from the positions of regular tetrahedra is shown in the left part of drawing in Figure 14. Now at the right side of <001> coordinate line there is shift of atom #2 upwards in the <001> direction, and atom #4 downwards in the <00-1> direction. If 1.57 Å will be assigned to the distance between atoms #2 and #4, then the distance between atoms #1 and #2, #1 and #4 will be 1.51 Å The same will be for pairs #2 and #3, and #3 and #4. This fits well to the positions of satellites on the both sides of the 111 Bragg reflection. The shifts proposed above are the most reasonable explanation for deformation of the regular tetrahedra at the twin <1-10> line. The shifts can be accommodated because the octants above, in the directions indicated by arrows, are empty. Unit cell of diamond can be divided for 8 octants; 4 octants are filled with tetrahedra and 4 octants are empty.

The deformation of tetrahedra around the line marked as <-110> is also a result of possible incorporation of foreign atoms in this area. The bonding network is seriously disturbed because atoms #2 and #4 have 5 C atoms in the first coordination sphere, instead of 4 C atoms in diamond structure. So, this coordination model is not realistic and needs to be modified, as shown above.

X-ray diffraction demonstrated that displacement disorder of atoms is real, so what is the cause of disorder? Let's consider that H atoms substitute some C atom along the line of twinned tetrahedra. The valence of H is 1, whereas is 4 for C atom, and any additional H atom, when incorporated, relaxes bonding configuration along the twin line, where 5 members coordination appears. The other contribution to the relaxation can come from vacancies and N atoms. PPG chemical analysis is not adequate in this case. Participation of N species in the growth process is a difficult issue to solve, but abstraction of HCN can appear. In any case, the distribution of atoms along the twin line is full of broken bonds and displacement disorder of atoms, because interatomic distances of C-C and C-H vary around. This disturbed area around <110> line can be represented by a long cylinder, but the matrix around is undisturbed. We associate the cylinder with threads in the arms of the cross. It seems to be situation similar to the interface between Si and HOD diamond film, where displacement of spots of HRTEM image is shown in a thin layer approximately 10 Å thick (Figure 7 in [1]). The spots correspond to complexes of atoms, not to individual atoms. They are not resolved in this particular image. Despite of the disturbance, caused by the different size of Si and C atoms, crystal fields of Si and diamond parts are adjusted, and the atomic order of the matrix is achieved. Similarly, in situation of a linear model, the matrix is uniform according to the long range order of atoms confirmed by x-ray diffraction.

The 3-dimentional model considers orthogonal linear defects arranged in layers parallel to the epitaxial plane. A single linear defect is shown in Figure 14. The linear defects alternate in <110> and <1-10> directions, whereas the growth proceeds in <001> direction. Within the linear defect, C atoms are displaced according to the distortions of the second kind (see [1]). The inter-atomic distances are described by a distribution with the main maximum at 1.54 Å, and associated maxima, on both sides, calculated from the positions of satellite reflections, such as 1.51 and 1.57 Å. These atoms are involved in disorder which has 3-dimentional distribution, similarly to diamond matrix. Therefore, x-ray diffraction taken with a circular collimator produces rounded spots. This description fits to the observed rounded spots. Does the growth process on (001) fit to our hypothesis? Certainly, it does; however, it is necessary to consider competitive hypotheses, but first exemplify facts which contradict the above hypothesis. These facts can emerge after comprehensive characterization of (001) epitaxial crystals. In contrast <111> epitaxy represent

different growth mechanism with planar defects. It results in diffraction spots are not rounded, but they form arcs instead.

Support for above conclusion comes from the comparison of the following diffraction patterns:

1. Oscillation and stationary patterns from Si and natural diamond do not show satellites (Figure 1A, 1B, 2A, 2B) in [1]. The Bragg spots are rounded because the x-ray primary beam is passed through the cylindrical collimator.

2. Stationary pattern from CVD (111) film grown on natural diamond facet shows a 111 cubic diamond reflection, satellite reflection at 2.12 Å, 3 streaks and a large spot. The Bragg spot and satellite are elongated according to arc. This is a completely different diamond defect structure from that of a natural crystal.

3. Oscillation and stationary patterns from (001) CVD single crystals show broadening, satellites and triplets around 111 (Figure 1, 2, 3, 4, 5). Shapes of satellites spots are rounded, similarly to the natural cubic diamond spots.

4. Conclusions

Single crystals of CVD diamonds (from jewelry store) grown with N_2 addition to microwave plasma were studied by X-ray diffraction oscillation and stationary crystal methods. Imaging plate area detector (IPA) of Rigaku revealed details in scattering in vicinity of reciprocal lattice points (rlp's). This scattering distinctly differs from that of natural diamond and departs from cubic symmetry. The interpretation of CVD crystals diffraction patterns based on approach developed in [1] indicates the presence of long and short range order in a diamond lattice. In this particular case, long range order means that crystal lattice is periodic and short range order means that ordering exists at small distances in limited areas.

Diamond diffraction from CVD crystals results in additional scattering around 111, 220 and 311 reflections. This scattering is superimposed on sharp peaks of Bragg reflections 111, 220, 311, 222, 400 and 331. Appearance of short range order as scattering in the vicinity of rlp requires explanation in terms of positions of atoms in disturbed diamond lattice. These positions are shifted from the nodes of ideal diamond lattice. A consideration of the existence of liner defects in <110> and <1-10> directions was conducted. The existence of a linear twin is presumed as a line where the tetrahedra share edge, it can cause atomic displacement from diamond lattice nodes in the range of 2% of interatomic distance, as was observed experimentally. Working with hypotheses is inevitable in this study, but in future aberration corrected high-resolution TEM images are believed to reveal atomic configuration of lattice defects in (001) epitaxial crystals.

The linear <110> twin, as shown in Figure 14, need to be modified in a bonding pattern network to fulfill the requirement of tetrahedral coordination of carbon atoms. The suggestion is that a stable configuration along the linear defect should have on average 8 valence electrons per atom pair. Such modification is possible by substitution of some carbon atoms by hydrogen atoms or/and by vacancies. The shifts of atoms in the vicinity of <110> linear defect correspond to satellite reflections of 111 Bragg peak. The peak which relates to 111 interplanar distance of 2.10 Å corresponds to 1.57Å of interatomic distance between carbon atoms in tetrahedron. The satellite peak at higher θ corresponds to 2.02Å. The interatomic bonding distance is 1.51Å, compared to 1.54Å for cubic diamond. The existence of atomic pairs with interatomic distances in the range like above describes the specific situation of studied CVD crystals.

The CVD (001) diamond single crystals, grown in the presence of nitrogen, represent a new class of diamonds which are different than natural and HP/HT crystals with respect to defects. They also have different x-ray diffraction patterns than other growth sectors of CVD crystals.

5. Highlights

X-ray diffraction from CVD diamond single crystals gem quality revealed lattice disorder.

Diffuse scattering around reciprocal lattice points was measured with image plate detector.

Hypothesis about linear growth defect is based on the concept of tetrahedra sharing edges.

Lattice distortions of the first and second kind were identified in diffraction patterns.

1500 cm^{-1} band in Raman spectra of disordered diamond was assigned to planar defects.

Acknowledgements

This report was supported by Penn State Materials Research Institute grant # UP31200. Mark Angelone is acknowledged for the help in collecting x-ray diffraction data. I am grateful for my late wife Teresa for her help in CVD growth research.

References

[1] Badzian, A. The displacement disorder of atoms in diamond crystals revealed by x-ray imaging plate detector, Diamond and Related Materials 2016, 69, 19-32

[2] Mierzejewska, S., Niemyski, T., J. Less-Common Metals 1966, 10, 33-37

[3] Badzian, A; Niemyski, T.; Appenheimer, S.; Olkusnik, E. "Graphite-Boron Nitride Solid Solutions" in F. A. Glaski, (Ed.), Proceedings of the Third International Conference on Chemical Vapor Deposition, Salt Lake City, April 24-27.

[4] Badzian, A., Cubic boron nitride – diamond mixed crystals (soild solutions), Materials Research Bulletin 1981, 16,1385-1393

[5] Badzian, A., Badzian, T., Lee, S.-Tong Synthesis of diamond from methane and nitrogen mixture, Appl. Phys. Lett. 1993, 62, 3432-3434

[6] Badzian, A., Recent developments in hard materials, Refractory Metals and Hard Materials, 1997 15, 3-12

[7] Badzian, A.; Badzian, T. Perpendicularly stacked graphite nanotubes, Carbon, 2000, 38, 1507-9.

[8] Locher, R, C. Wild, N, Herres, D. Beher, P. Koidl, Nitrogen stabilized <100> texture in chemical vapor deposition diamond films, Appl. Phys. Lett. 65, 1994, 34 – 36.

[9] Pickrell, D., R. Messier, R. E. W. Zhu, A. Badzian, R. Newnham "Downstream plasma-enhanced diamond film deposition, Appl. Phys. Lett. 56, 1990, 2010-2012.

[10] Ziminsky, P. How high quality synthetic diamonds will impact the market, Kitco Contributed Commentaries, Web page, July 12,2013

[11] Zhao, X-Z; Roy, K; Cherian, K. A; Badzian, A. Hydrothermal growth of diamond in metal-C-H2O systems, Nature 1997, 385, 513-515.

[12] Badzian, A; Badzian, T. Diamond homoepitaxy by chemical vapor deposition, Diamond and Related Materials 1992, 2, 147-157.

[13] Badzian, A.; Badzian, T.; Wang, X. H.; Hartnett, T. M. Growth Sectors of CVD Diamond, New Diamond Science and Technology, Materials Research Society: Pittsburg, Pennsylvania, 1991, pp.549-556.

[14] Badzian, A.; Badzian, T. Defects in CVD diamonds, Ceramic International, 1996, 22, 223-229.

[15] Erni, R.; Freitag, B.; Hartel, P.; Muller, H.; Tiemeijer, P.; van der Stam, M; Stekelenburg, M; Hubert, D;Specht, P; Garibay-Febles, V. Atomic scale analysis of planar defects in polycrystaline diamond, Microsc Microanal. 2006, 12,492-7.

[16] Badzian, A.; Badzian, T. An intermediate hybridization in diamond: edge-shared tetrahedra, Thin Solid Films 2004, 447-448, 163-168.

[17] Lee, N. Microwave plasma-assisted chemical vapor deposition and characterization of (001) homoepitaxial diamond films, PhD Thesis, The Pennsylvania State University, May 1996.

[18] Kuang, Y. Study of growth and nucleation of chemical vapor deposition diamond and amorphous silicon carbon alloy thin films, PhD Thesis, The Pennsylvania State University, May 1997.

[19] Kuang, Y.; Wang, Y., Lee, N.; Badzian, A.; Badzian, T.; Tsong, T. T. Surface structure of homoepitaxial diamond (001) films, a scanning tunneling microscopy study, Appl. Phys. Lett. 1995, 67, 3721-3723.

[20] Kuang, Y.; Lee, N.; Badzian, A.; Tsong, T. T.; Badzian, T.; Chen, Ch. Study of antiphase boundaries local 3x1 configuration on the (001) surface of homoepitaxial diamond films by scanning tunneling microscopy, Diamond and Related Materials, 1995, 4, 1371-1375.

[21] Badzian A. Synthesis of diamond from the gas phase, Electric Refractory Materials: Marcel Decker, New York, NY, 2000, pp. 347-368.

[22] Grot, S. A.; Gildenblat, G. Sh.; Hatfield, C. W.; Wronski, C. R.; Badzian, A.; Badzian, T.; Messier, R. The effect of surface treatment on electrical properties of metal contacts to boron-doped homoepitaxial diamond films, IEEE Electron Device Lett. 1990, 11, 100-102.

[23] Stallcup, R. E.; Avies, A. F.; Perez, J. M. Atomic resolution ultrahigh vacuum scanning tunneling microscopy of epitaxial diamond (100) films, Appl. Phys. Lett. 1995, 66, 2331-2333.

[24] Hutchison, J. L; Shechtman, D. High resolution electron microscopy of CVD diamond film, Advanced Materials '94, International Communications Specialists, Inc.:Tokyo, 1994, pp. 152-156.